Microstructure-Sensitive Thermomechanical Forming Simulation Capability

L. Borkowski, M. Anahid, and A. Staroselsky*
Raytheon Technologies Research Center
411 Silver Lane, East Hartford, CT, USA 06118
*Corresponding author: alexander.staroselsky@rtx.com

Keywords: Thermomechanical; Crystal plasticity; Large deformation; Finite element; Shear band

ABSTRACT

A novel modeling capability has been developed which permits consideration of metallic microstructure evolution in thermomechanical forming analyses. Specifically, the evolution of microstructural features such as crystallographic texture and grain constitutive response are predicted using a large deformation crystal plasticity model. This is coupled with the state-of-the-art remeshing/adaptivity capabilities in commercial finite element software LS-DYNA. By allowing remeshing and properly remapping the microstructural features to the new mesh, the modeling framework is able to simulate significantly larger local deformation (greater than 900% strain) than traditional crystal plasticity finite element. Thus, the developed model permits large deformation forming operations such as forging to be simulated, yielding output which includes the final microstructure as well as the analysis of shear band localization and appearance of localized damage. The model has been calibrated and successfully applied to the high temperature forging of Al-Li 2070 (fan blade material) into complex geometries. The generalized nature of the model allows its further application to a wide range of thermomechanical forming processes and material systems.

1. INTRODUCTION

There have been considerable recent advancements in understanding and predictive modeling of material processing at high temperatures. At the same time, manufacturing technology and equipment have also dramatically improved in speed and capability for thermomechanical processing which combines plastic deformation with thermal control for non-isothermal regimes and at various rates, such as during forging, rolling, and extrusion operations. Technological progress sets new challenging tasks for the mechanics of materials community. Special interest has arisen in manufacturing light weight and strong parts which is a critical step in production of aerospace components. Accurate predictions of material response for large plastic deformations are complex and greatly compounded during high temperature material processing. Many factors affect the strength and damage initiation and propagation in the parts, the most important of which are microstructural effects, such as grain size and shape and crystallographic texture. In the modern industrial world, forging plays a critical role in producing parts that are stronger than ones obtained by other methods. It uses polycrystalline metal grain plastic flow to shape the required geometry while increasing the yield value due to strain hardening. At the same time forging avoids metal cutting or casting that breaks the natural grain structure. Therefore, the accurate prediction of anisotropy due to crystallographic texturing becomes crucial.

Parts resulting from thermomechanical processing operations such as forging contain heterogeneous microstructure due to location-specific deformation history. Since part performance and life is controlled by microstructure (Yeratapally et al., 2016; De et al., 2009; Shassere et al., 2018), prediction of its evolution throughout and final microstructure following processing is a key component of a comprehensive process-property predictive simulation framework. Relevant microstructure features include texture, grain size and morphology, and accumulated strain in the grains. Because of the importance of simulating large-deformation

processes to predict as-produced properties, several research efforts have been focused on this goal (Kalidindi et al., 1992; Glavicic et al., 2008; Knezevic et al., 2009). Kalidindi et al. (1992) applied a Taylor-type polycrystalline model, integrated with a finite element solver, to the forging of a billet yielding heterogeneous deformation. The model performed well in predicting the location-specific texture for the limited global deformation permitted without remeshing. Integrating the Los Alamos polycrystalline plasticity (LApp) code with DEFORM, Glavicic et al. (2008) analyzed texture evolution in a two-phase titanium alloy during forging. In their approach, the finite element analysis (FEA) forging simulation was run and the resulting integration point strain increments and metal-flow-related rotations were fed into the LApp code for subsequent texture prediction. In (Knezevic et al., 2009), discrete Fourier transform (DFT) was employed to represent all the functions necessary to perform crystal plasticity simulations. The model was applied to various case studies including an equi-channel angular extrusion where the heterogeneous deformation field in the isotropic material was extracted and post-processed using the DFT crystal plasticity model to predict texture. An underlying thread between several of these models is the application of crystal plasticity theory to account for deformation at the grain level in polycrystalline alloys.

Currently, crystal-plasticity finite element (CPFE) models allow predicting the effect of local microstructure, resulting from specific forming operations, on the mechanical behavior of parts. Crystal plasticity theory provides the necessary link between macroscale and microscale deformation, governed by the relevant physical mechanisms. Specifically, it allows resolving the globally applied deformation and subsequent stress to the individual slip systems in the polycrystalline microstructure and computing the resulting deformation driven by dislocation motion. Integrated with a finite element software, the CPFE model allows coupling work-piece loads, boundary conditions, and heterogeneous deformation with grain-level plasticity and resulting microstructural evolution. It is for this reason that CPFE is often called upon to simulate thermomechanical processing involving large deformations (Kalidindi et al., 1992; Glavicic et al., 2008; Knezevic et al., 2009; Si et al., 2008) in addition to high temperature creep (Staroselsky and Cassenti, 2010; Deka et al., 2006) and fatigue (Anahid et al., 2011; Prithivirajan and Sangid, 2018). While most crystal plasticity formulations are based on large deformation mechanics, the total deformation capability of the CPFE model is limited by mesh quality in the finite element model.

Often model applicability is limited by the inability of FEA to simulate large deformation without remeshing. While many commercially-available FEA software packages provide remeshing capabilities, none are able to perform tightly coupled multiscale simulations with remeshing. This in turn limits the types of simulations which can be performed with remeshing. This paper presents the development and validation of a robust FEA-based model capable of remapping solution and user-defined state variables in order to predict location- and microstructure-specific part properties resulting from forging operations. To accomplish this, a computational multiscale model was coupled with advanced adaptivity/remeshing to yield a microstructure-sensitive forging simulation capability for large deformation operations. The developed model is first-of-its-kind and will facilitate optimized process design while yielding parts with improved properties and reduced weight.

Remeshing is a necessary component of the developed model. Distorted finite element meshes can degrade element accuracy and reduce convergence rate (Belytschko et al., 2013). Furthermore, mesh distortion can cause an element to invert, leading to a negative Jacobian and ultimate failure of the solution procedure. Therefore distorted meshes, either due to excessive shear or normal deformation, are to be avoided. However in large deformation simulations, local strain can exceed several hundred percent. Elements subjected to this magnitude of deformation will inevitably become distorted. To address this issue, several commercial finite element packages provide remeshing or adaptivity capabilities that can be utilized in simulating large deformation operations (e.g., mesh nonlinear adaptivity in ANSYS, adaptive remeshing in Abaqus, 3D adaptivity in LS-DYNA). Some specialized software (e.g., DEFORM) provide the ability to account for microstructure while also permitting large deformation through remeshing. This capability allows the user to predict the as-produced

microstructure as a function of the deformation history throughout the work piece. One method employed by DEFORM to provide this coupling is predicting the microstructure in post-processing which entails only one-way coupling between deformation and texture. Ideally in these simulations two-way coupling should exist where deformation affects texture and vice versa, especially for highly-textured parts. Using another approach, DEFORM provides this two-way coupling in a simplified manner by using a calibrated crystal plasticity model to fit an anisotropic yield surface (e.g., quadratic Hill model (Hill, 1948)) and flow rule which can be called during the forging simulation. Although this method permits efficient execution by reducing the crystal plasticity problem into one that can be solved using classical plasticity, microstructural information and accuracy is sacrificed. This is in part due to the fact that DEFORM uses conventional remapping techniques to transfer texture information during remeshing which is discrete in nature.

To address the deficiencies in current state-of-the-art thermomechanical forming simulation capabilities, a model is developed which couples, directly in a two-way fashion, microstructure evolution and finite element remeshing. This two-way coupling between deformation and microstructural evolution will enable more physically accurate (i.e., representative) simulations, especially for large deformation scenarios. A schematic of the components comprising this model is shown in Figure 1. As depicted in this schematic, the goal of the effort presented herein is to provide an accurate model to predict the effect of processing on part properties. This model is applied to a forging operation yielding heterogeneous microstructure while validation is conducted based on location-specific texture prediction.

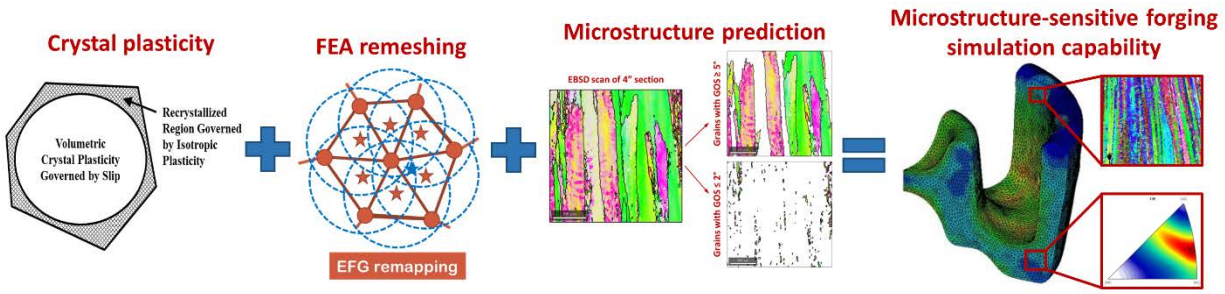

Figure 1. Schematic showing the components of the microstructure-sensitive forging model

2. 3D ADAPTIVITY AND REMAPPING TECHNIQUE

Metal forging analysis involves large material deformation where mesh distortion often leads to numerical instability and inaccurate stress prediction. The 3D adaptive process in LS-DYNA helps to improve the mesh quality through tetrahedron-based remeshing. Remeshing operations can be split into three basic steps: (i) the remeshing decision; (ii) the new mesh generation; and (iii) the accurate transfer of data from the old mesh to the new mesh.

The remeshing decision is normally controlled by error estimates based on the stress or strain error norms computed in the finite element mesh or by the use of distortion criteria characterizing the geometric distortion of the elements. After remeshing, all nodal and integration point quantities must be remapped from the old mesh to the new one. Remapping is a critical component of adaptivity since error can be introduced and information lost if done incorrectly. Currently in LS-DYNA, two methods exist to remap field quantities following remeshing: FEM and element free Galerkin (EFG). Element-free Galerkin remapping (Wu and Lu, 2009; Lu and Wu, 2006) is developed with high-order accuracy and smoothness which can minimize the numerical error associated with transferring the continuous deformation and stress fields from the old to the new mesh. It has

been demonstrated that the EFG remapping approach is preferred over FEM based on its ability to preserve information and maintain gradients in fields such as stress and strain (Wu and Lu, 2009; Lu and Wu, 2006).

However, while these approaches can be applied to remap FEA field variables (e.g., displacement, stress, strain), they are unsuitable for microstructural variables such as texture. In contrast with a conventional phenomenological plasticity model, the CPFE material model calculates the material response based on the evolution of micro-grain structures, where the material history variables are discrete by natural. Therefore, new remapping schemes must be developed to transfer the discrete information of collective micro-grain structures from the old material points of the FE mesh to the new ones. Once developed, these remapping schemes can be employed to extend the 3D adaptivity capabilities in LS-DYNA.

2.1. Remapping schemes for CPFE material model

Following remeshing, the Gauss point parameters have to be transferred to the nodes in the current deformed mesh. Once the state parameters are available at the old mesh nodes as a result of smoothing, these have to be transferred to the Gauss points of the new mesh. As a result, interpolation smoothing of the field variables takes place. This is a perfectly acceptable procedure for remapping continuous parameters, however for discrete state variables, smoothing could lead to erroneous results. For example, let us recall that the local properties of the material depend on the crystallographic orientation of individual grains. Now assume, for the sake of simplicity, that initially each finite element corresponds to one grain. After remeshing, for example, two original grains might span three new elements. As a result of smoothing transformation of the parameters in this hypothetical case, the third element with intermediate grain orientation would be generated. This adds to the system a non-existing grain (or number of grains), principally changing crystallographic texture and subsequently anisotropic properties of the material. Hence, the standard “smoothing” remapping algorithms cannot be used for remeshing discrete parameters such as grain orientations and related values.

The micro-grain structures in CPFE are different from point to point in the continuum scale, which leads to a discrete distribution of the CPFE material variables among integration points (IPs) of finite elements. In order to maintain the sharpness of such a discrete distribution, instead of a smoothing algorithm, the CPFE material variables of a new IP are set to those of one particular old IP by two different methods: closest point projection (CPP) and Monte Carlo (MC). These alternative approaches can be described as follows. Closest point projection is a numerical scheme to compute coordinates of a point projected onto a surface. For any given new IP, there are a set of old IPs with meshfree supports covering it as shown in Figure 2. Within the set of points, the CPP method simply identifies the point with the shortest distance to the new IP and transfers its CPFE material variables to this new IP. Specifically in this application, the radius of influence is defined and the value of discrete state variables (e.g., crystal orientation) and related parameters are projected from the original mesh onto new mesh integration points. A disadvantage of this approach is that it may result in too sharp of a microstructure driven by few integration points.

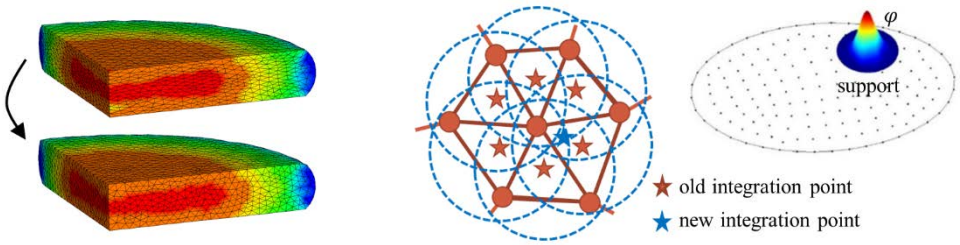

Figure 2. Remapping internal variables at integration points

The MC method, on the other hand, uses the sampling from a probability distribution in the set of neighboring old IPs. The remapping process is treated as a stochastic sequence of the local transformations of each element. Thus, the probabilities of local transformations developing per unit of time are defined in the framework of transition-state theory as follows: $\omega = \omega_0 \exp\left(-f(r/r_0)\right)$, where r is the distance of the old integration points from the new one, r_0 is a normalization factor, and ω_0 is the pre-exponential frequency factor. We specify a given integration point from which we map the state variables by corresponding set of probabilities for each set of old mesh integration points within some distance, $r \leq R$. The probability of choosing an integration point for mapping its parameters decreases with the distance from the new integration point to which the properties will be remapped. The total rate for original mesh integration point choice determines the overall probability rate, which is the sum of all rates over all mesh elements in the chosen area around the new integration point, i.e.: $W = \sum_{\substack{mesh\ elements \\ r \leq R}} \omega(IP\ of\ old\ mesh)$.

The choice of the element or integration point for mapping at this step is based on the contributions of each individual probability to the total rate W. The normalized probability rate for each possible choice may be written in the form: $\chi_i = \frac{\omega_i}{W}$ where $\sum \chi_i = 1$. The second relationship implies that one of the integration points would be always chosen. Next, we use a kinetic Monte-Carlo simulation for choosing the location of the next source integration point by generating a random number ξ uniformly distributed in the interval (0,1). All χ_i are aligned one after another along the interval (0,1). The i[th] interval in which the random number falls is chosen as the source microstructure for remapping. This process is illustrated in Figure 3. Naturally, the probability of choosing interval [i, i+1] linearly increases with the increase of its length χ_i.

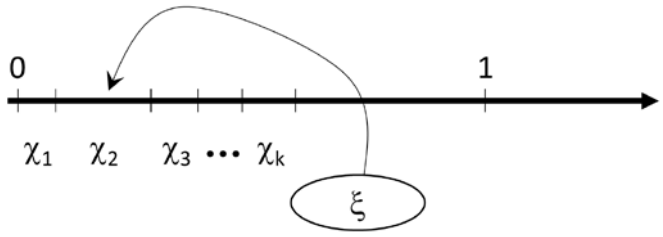

Figure 3. Scheme of Monte-Carlo process

In this work, the probability of choosing a specific old IP with coordinates X_j follows a Gaussian distribution function defined by its support size a_j and distance to the new IP with coordinates x

$$\omega_j(x, X_j) = \frac{e^{-|x-X_j|^2/a_j^2}}{\sum_{j=1}^{NP} e^{-|x-X_j|^2/a_j^2}}. \quad (1)$$

Further discussion of the two remapping techniques, CPP and MC, is provided in Ref. (Borkowski et al., 2021). In this discussion, different scenarios are investigated and each of the remapping techniques evaluated.

3. FORGING EXPERIMENTS AND SIMULATION

Combination of the crystal plasticity model described in Staroselsky and Borkowski (2019) with the microstructure-appropriate adaptivity remapping technique presented in Section 2 yielded a model suitable for simulating large deformation operations such as forging. In typical forging operations, heterogeneous deformation fields lead to spatial variation of the evolving microstructure. Therefore tests were designed to be

representative of a realistic forging process. In particular, a die geometry was designed such that a heterogeneous microstructure would result. Following forging testing and microstructure characterization, the developed model was called to simulate the process. Textures were extracted from both the experimental and simulation forged parts and comparisons made.

3.1. Forging testing and microstructure characterization

Forging experiments were carried out using a channel die testing apparatus as shown in Figure 4. For these tests, a 1.27 cm (0.5 in) cube specimen of Al-Li 2070 was compressed in a channel to provide plane strain conditions (Figure 4a). This allowed the compressed specimen to fill up the voids in the elliptical punch (Figure 4b) while maintaining a 2D strain state. The tests were performed in a clam-shell oven with thermocouples placed against the specimen to monitor the temperature (Figure 4c). In addition, boron nitride lubricant was applied to the channel and die surfaces to minimize friction at the high forging temperatures.

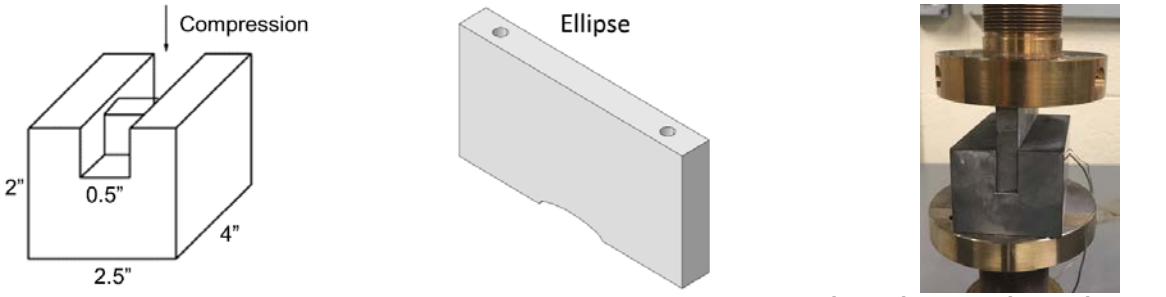

a) Channel die apparatus geometry and specimen

b) Forging punch ellipse geometry

c) Forging experimental setup

Figure 4. Channel die forging setup

Following the tests, each specimen was sectioned along its central plane and EBSD performed at four locations, denoted Site A through Site D in Figure 5. These four sites were chosen in order to quantify the location-specific microstructure and texture as a result of the heterogeneous deformation caused by the ellipse die geometry.

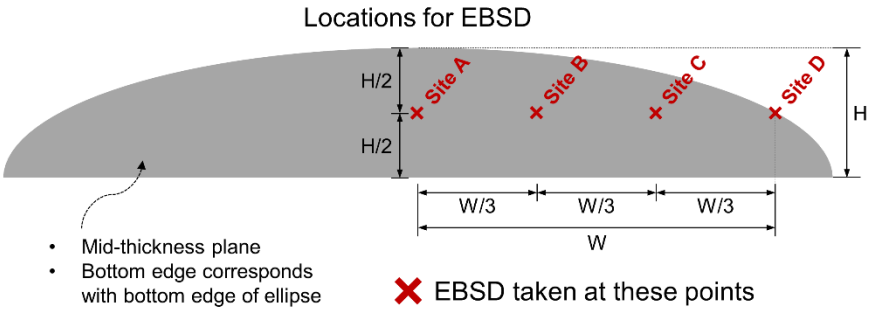

Figure 5. Channel die forging microscopy locations

The 1.27 cm (0.5 in) cube billet was extracted from the mid-thickness, mid-plane of the 10.16 cm (4 in) location of an H-beam forging (Borkowski and Staroselsky, 2018). The microstructure, obtained via EBSD, is represented as an inverse pole figure map in Figure 6. It can be observed that the grains are elongated in the L direction due to prior forging operations. Furthermore, the billet texture is shown in Figure 7. This texture is presented with the z-axis (coming out of the page) representing the plane-constrained axis from the forging tests

and simulations. The forging operations leading to this microstructure as well as the resulting texture were predicted in (Borkowski and Staroselsky, 2018) using CPFE. The initial microstructure for the forging simulations will be sampled from the data presented in Figure 6 and Figure 7.

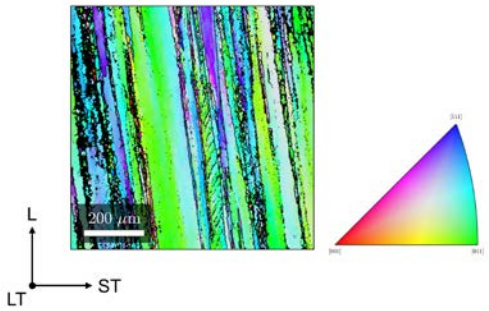

Figure 6. Initial billet microstructure

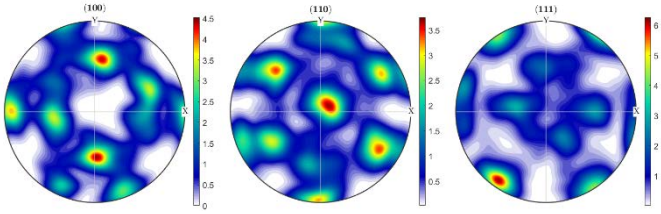

Figure 7. Initial texture for ellipse forging simulation; pole figures looking down channel die constraint axis

3.2. Forging model and validation

Given the large strains experienced during the laboratory forging test, it is likely that simulating such an operation would be difficult without employing adaptivity. This is especially true if a crystal plasticity model, which requires the deformation gradient as input, is being called at every integration point in the model. To test the limits of the LS-DYNA forging model with the crystal plasticity subroutine but without remeshing, a simulation of the ellipse forging was performed. In this simulation, a symmetric Al-Li 2070 billet was deformed in compression until model failure occurred. The simulation ran to approximately 60% global engineering strain until the crystal plasticity model failed to converge. At this strain, the elements along the boundary of the ellipse die were severely distorted with aspect ratios much larger than one.

In order to run the forging simulation to completion and obtain the forged texture, it is obvious that remeshing must be included with the crystal plasticity LS-DYNA model as described in Section 2. Therefore subsequent models employed this coupled approach for simulating the forging of an Al-Li 2070 billet with an ellipse die as shown in Figure 8. The full 3D billet is meshed with 17,152 tetrahedron solid elements while the rigid top and bottom dies are meshed with 2D shell elements. Contact is enforced between the billet and the top and bottom dies. The through-thickness displacements on the front and back faces of the billet are constrained to enforce plane strain conditions. In order to replicate the corresponding experiments, a global/forging displacement rate of 4.67e-2 cm/s (0.0184 in/s) was applied to the top die. This loading rate corresponds to a strain rate of 1e-1/s. The forging simulation was performed at the same temperature as the experiments, 371 °C (700 °F). In the model, pressure smoothing was employed to alleviate issues arising from the incompressibility of the plastically deforming material. Finally, the model was solved using an implicit solver.

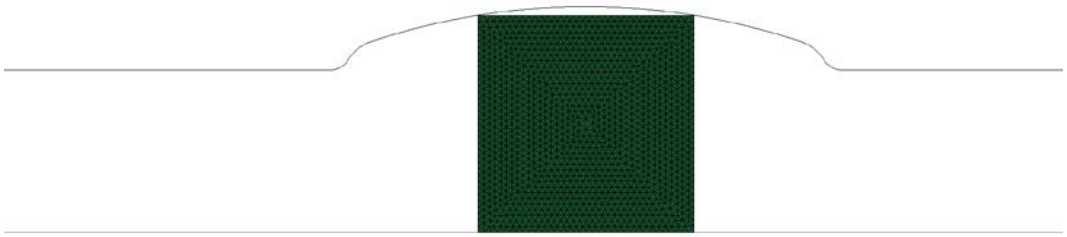

Figure 8. Original billet mesh and ellipse die for forging simulation

Coupling the CPFE model with 3D adaptivity allows the material constitutive response and microstructural evolution to be determined by crystal plasticity theory while permitting large deformation operations to be performed. Following compression to a global strain of 92.5%, the heterogeneous deformation can be observed in the deformed mesh as seen in Figure 9. During this particular simulation, remeshing was performed adaptively based on the shear strain criterion (Hu et al., 2010). Remeshing was activated a total of 16 times through the simulation starting at approximately 50% global strain. The option for local mesh refinement was implemented to allow for a finer mesh in areas of greater curvature such as around the corner at both ends of the ellipse geometry as shown in Figure 9. Based on the results presented in Section 2, the CPP remapping scheme was employed.

Figure 9. Final deformed mesh from ellipse forging simulation

Once the forging model was run to completion, the location-specific texture could be investigated. The experimental and predicted texture from Site A, B, C, and D are presented in Figure 10, Figure 11, Figure 12, and Figure 13, respectively. In each of these figures, the top pole figure represents the experimental texture while the bottom one is the predicted texture. Comparing the experimental textures at the four locations, the variability in deformation history and microstructural evolution from the original texture presented in Figure 7 is evident. These four locations therefore represent a good test for the capabilities of the developed modeling framework. The post-forged simulated microstructures appear to match well with the corresponding experimental microstructures. Specifically, nearly all the major texture components represented in the pole figures from the four locations are predicted correctly. The discrepancies between the experimental and predicted textures can be in part attributed to slight mismatches in locations of texture extraction between EBSD and model. In addition, as mentioned in Section 2, microstructural information can be lost during remapping following remeshing. It was for this reason that the number of remeshing steps was minimized. However, the benefit of being able to simulate the large deformation forging operation while considering microstructural evolution outweighs the possible inaccuracies introduced through remapping. The magnitude of error introduced due to remapping following remeshing was quantified in Ref. (Borkowski et al., 2021).

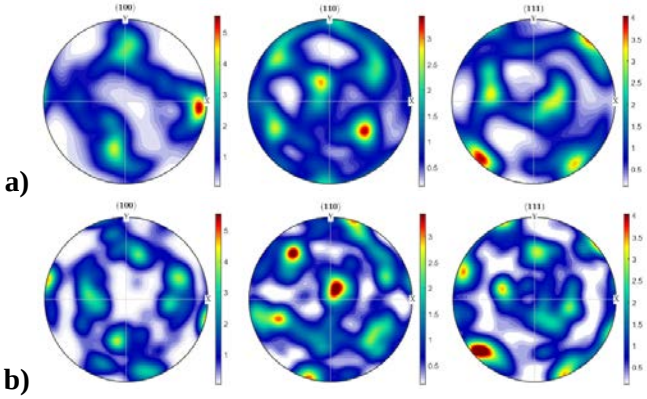

Figure 10. Texture comparison at Site A: a) Experimental texture; b) Simulation texture with remeshing

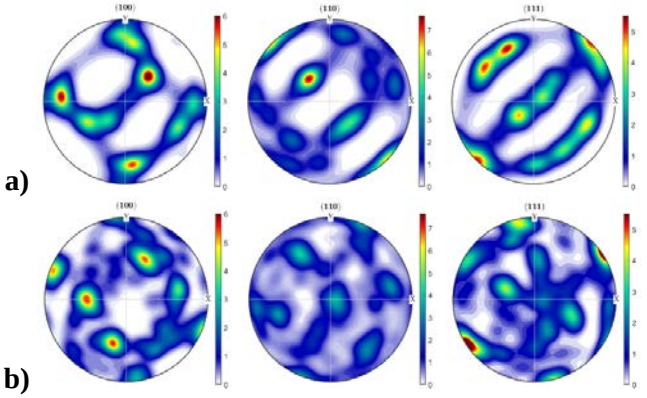

Figure 11. Texture comparison at Site B: a) Experimental texture; b) Simulation texture with remeshing

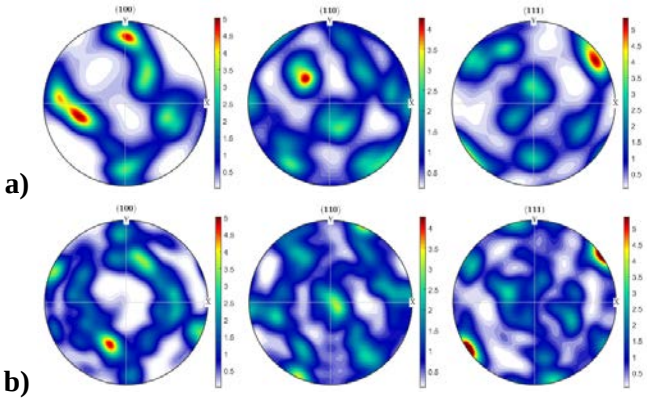

Figure 12. Texture comparison at Site C: a) Experimental texture; b) Simulation texture with remeshing

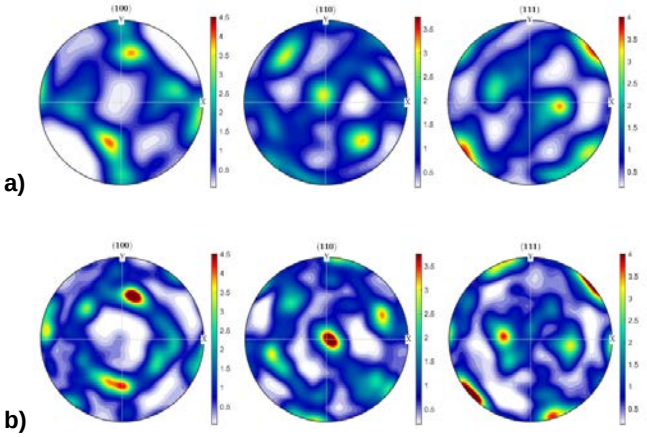

Figure 13. Texture comparison at Site D: a) Experimental texture; b) Simulation texture with remeshing

The benefits of coupling a crystal plasticity model with remeshing for large deformation simulation extend beyond allowing for texture prediction. Another microstructure-dependent history variable that can provide valuable insight into the material local deformation includes the equivalent plastic strain, defined in Eq. (2). Since each grain in the RVE assigned to each element will have a unique value of plastic deformation gradient (F^P), the scalar value of the equivalent plastic strain (E^P_{eq}) must be volume averaged at each integration point. This is the same procedure that is employed for computing integration point stress. It is therefore the mean equivalent plastic strain (averaged over the relative volumes of the associated grains) that is provided as a history variable for output.

$$E^P_{eq} = \sqrt{\frac{2}{3}[(E^P_{11} - E^P_{22})^2 + (E^P_{22} - E^P_{33})^2 + (E^P_{33} - E^P_{11})^2 + \\ + \frac{3}{2}({E^P_{12}}^2 + {E^P_{23}}^2 + {E^P_{13}}^2)]} \tag{2}$$

where

$$E^P = \frac{1}{2}({F^P}^T F^P - I) \tag{3}$$

In many materials, inelastic strain can be concentrated spatially in a thin strip known as a shear band where the equivalent strain is perhaps up to an order of magnitude higher than the average strain in the material (Batra and Kim, 1992). This phenomenon is especially prevalent in materials which experience strain softening. As demonstrated in Ref. (Borkowski and Staroselsky, 2018), Al-Li 2070 does experience softening under compression at the forging temperatures. Because of this, when an instability forms due to shear, it will propagate along a thin band of elevated shear stress. This phenomenon can be observed in Figure 14 where the contour of equivalent plastic strain is plotted at various forging strain levels up to the final strain level of 92.5%. The formation of the shear band is evident in the center of the billet creating a V-shape of elevated plastic strain. Inspecting the final contour at 92.5% forging strain, the plastic strain in the shear band is at or above 900%. This magnitude of deformation is incredibly difficult to simulate accurately without remeshing since the elements in the shear band would be severely distorted. Therefore, the capability afforded by the developed forging simulation framework allows simulating such large strains while having access to microstructural-dependent history variables such as equivalent plastic strain.

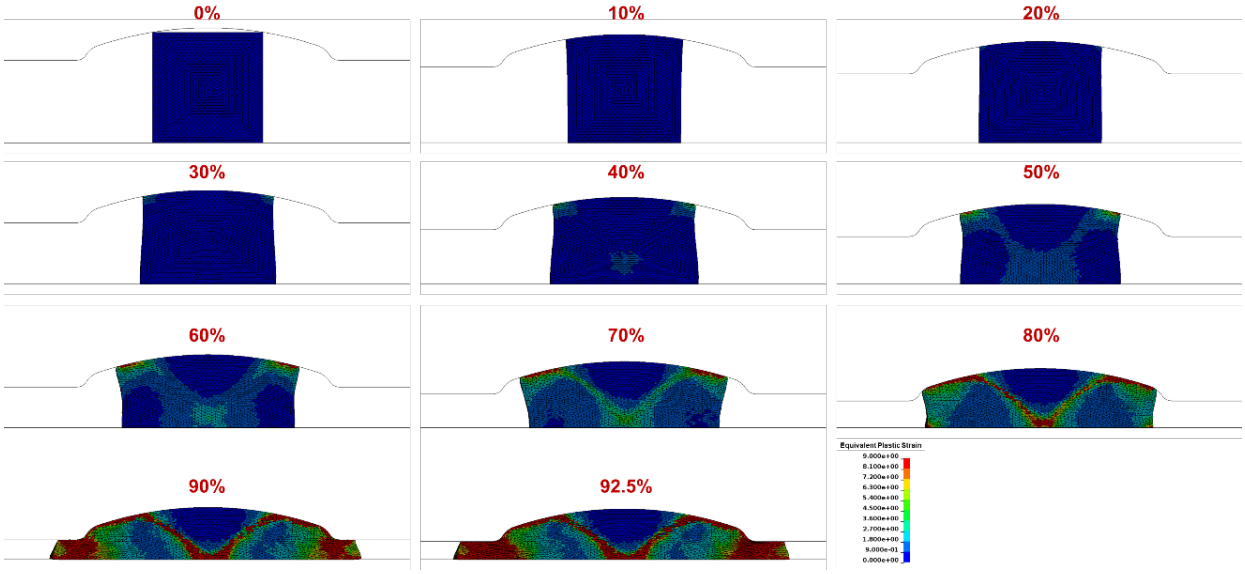

Figure 14. Equivalent plastic strain contours at various global forging strains

Looking more closely at the final contour in the series of forging steps presented in Figure 14, the cause and microstructural effect of the shear bands can be investigated. Toward this purpose, the equivalent plastic strain, displacement vector plot, and optical micrograph of the forged ellipse are presented at the same global strain level in Figure 15a, b, and c, respectively. Besides the shear band region in Figure 15a, elevated plastic strain can be observed near the ellipse outer boundaries as well as in the flash where the constrained material is forced through an increasingly narrow gap. The vector plot of displacement shown in Figure 15b lends insight into the macroscale deformation contribution to shear banding. Observing the direction and magnitude of the deformation on both sides of the shear band, denoted with white curves, it can be seen that there is a sudden change in the direction of displacement. For instance, inside/above the V-shaped shear band, the deformation is primarily downward indicating that the material in this region is undergoing unidirectional displacement due to the constraints placed on it by the ellipse die. Outside the V-shaped shear band, the material is flowing both outward and downward toward the opening between the dies. Therefore toward the top of the shear band, the motion is downward and outward whereas near the bottom, the flow is almost entirely outward. The nearly 90 degree change in flow contributes to the shear band formation. Finally, the plastic strain contour and displacement vector plot can be compared with an optical micrograph of the forged specimen (Figure 15c) to draw a connection between the deformation and final grain morphology. In this figure, the shear band is also denoted with white curves. Recalling that the grains in the original billet were elongated vertically (Figure 6), the multiaxial motion of the grains is evident from Figure 15c. For example, as reflected in Figure 15b, the grains along the centerline (horizontally) of the ellipse are primarily deformed vertically which is in agreement with the grain orientation in Figure 15c. Also evident is that the shear band corresponds to the regions where the grains experience a kink due to the sudden change in deformation. In addition to prediction of location-specific texture and plastic deformation, the model was shown to predict the load versus displacement response for the ellipse forging operation (Borkowski et al., 2021).

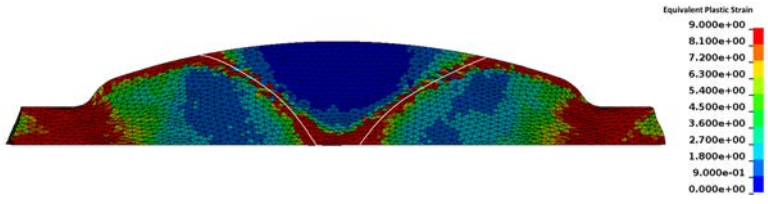

a)

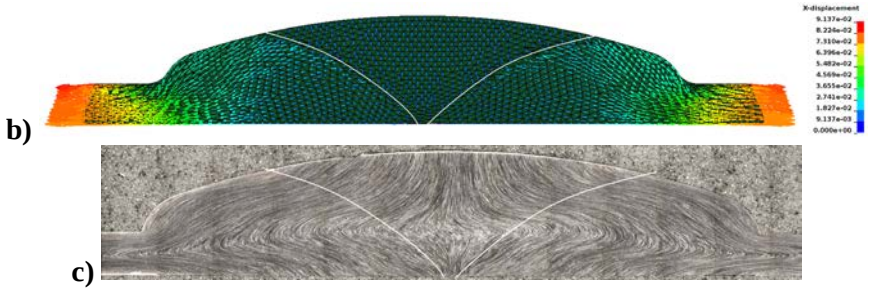

Figure 15. Connection between forged microstructure and simulation results: a) Inelastic strain contour with shear band denoted with white curves; b) Displacement vector plot with sudden directional flow change denoted with white curves; c) Optical micrograph of forged ellipse with region of grain direction change denoted with white curves (note that original grains were elongated vertically as shown in Figure 6)

4. CONCLUDING REMARKS

The overall objective of this work was to develop and validate a robust, physics-based model capable of predicting forged microstructures to guide processing optimization of parts for better performance, less weight, and longer life. Accomplishing this objective required the following: a microstructure-sensitive material model, tight coupling with FEA remeshing, and appropriate remapping techniques. The result was a model capable of assessing the influence of manufacturing process history on part anisotropic response up to several hundred percent inelastic strain. The integrated framework includes synergy of constitutive modeling, computational tool development, remeshing and remapping within a commercial FEA software, and experimental validation.

Forging of polycrystalline alloys leads to large anisotropic deformation, texture development, and adiabatic shear banding. Computational tools are needed to connect forging-related processing parameters to part microstructural characteristics and subsequent mechanical properties. Therefore, a physics-based, non-isothermal, viscoplastic crystal plasticity model has been unified with a probabilistic-based remeshing routine preserving crystallographic orientation of the deformed RVE and accurately mapping corresponding model state variables onto the new mesh. The calibrated model has been validated against laboratory forging experiments. Validation includes predicting the constitutive response of the material and final microstructure of a forged Al-Li part, which qualitatively agrees with experimental measurements.

The capabilities afforded by this unique model will allow tighter coupling between process and property prediction. Having a model which can predict microstructural evolution throughout the forming process can aid in designing improved processes which will yield parts with known heterogeneous microstructures with less variability. Finally, connection between the microstructure and resulting properties (e.g., creep, fatigue) can be achieved using physics-based techniques. Therefore, the presented model can play a key role in improving the performance and life of thermomechanical-processed parts. For example, such a tool could provide the as-received microstructure, following processing, as input to a microstructural-sensitive lifing model. Furthermore, certain microstructures and grain orientations are preferred in specific locations of a part such as a fan blade. Thus, the presented microstructural-sensitive, large-deformation model could guide the process design to yield such desirable location-specific microstructures. Because of the generality of the developed technique, extension of the model to other large-deformation operations such as rolling or extrusion would be straightforward, including calibration of the constitutive models to other materials and temperatures.

5. ACKNOWLEDGEMENTS

The authors are grateful for support and funding from Leading Innovations for Tomorrow (LIFT), operated by the American Lightweight Materials Manufacturing Innovation Institute (ALMMII).

6. REFERENCES

Anahid, M., Samal, M.K. and Ghosh, S., 2011. Dwell fatigue crack nucleation model based on crystal plasticity finite element simulations of polycrystalline titanium alloys. *Journal of the Mechanics and Physics of Solids*, *59*(10), pp.2157-2176.

Batra, R.C. and Kim, C.H., 1992. Analysis of shear banding in twelve materials. *International journal of plasticity*, *8*(4), pp.425-452.

Belytschko, T., Liu, W.K., Moran, B. and Elkhodary, K., 2013. *Nonlinear finite elements for continua and structures*. John wiley & sons.

Borkowski, L.B. and Staroselsky, A., 2018, March. Multiscale Model for Al–Li Material Processing Simulation Under Forging Conditions. In *TMS Annual Meeting & Exhibition* (pp. 355-364). Springer, Cham.

Borkowski, L., Anahid, M., Staroselsky, A., and Hu, W., 2021. Microstructure-sensitive large-deformation model for thermomechanical processing simulations. *International Journal of Solids and Structures*, *230*, pp.111161.

De, P. S., Mishra, R. S., & Smith, C. B. (2009). Effect of microstructure on fatigue life and fracture morphology in an aluminum alloy. *Scripta Materialia*, *60*(7), 500-503.

Deka, D., Joseph, D.S., Ghosh, S. and Mills, M.J., 2006. Crystal plasticity modeling of deformation and creep in polycrystalline Ti-6242. *Metallurgical and materials transactions A*, *37*(5), pp.1371-1388.

Glavicic, M.G., Goetz, R.L., Barker, D.R., Shen, G., Furrer, D., Woodfield, A. and Semiatin, S.L., 2008. Modeling of texture evolution during hot forging of alpha/beta titanium alloys. *Metallurgical and Materials Transactions A*, *39*(4), pp.887-896.

Hill, R., 1948. A theory of the yielding and plastic flow of anisotropic metals. *Proceedings of the Royal Society of London. Series A. Mathematical and Physical Sciences*, *193*(1033), pp.281-297.

Hu, W., Wu, C.T. and Saito, K., 2010. LS-DYNA meshfree interactive adaptivity and its application. In *11th International LS-DYNA Users Conference, Detroit* (pp. 10-21).

Kalidindi, S.R., Bronkhorst, C.A. and Anand, L., 1992. Crystallographic texture evolution in bulk deformation processing of FCC metals. *Journal of the Mechanics and Physics of Solids*, *40*(3), pp.537-569.

Knezevic, M., Al-Harbi, H.F. and Kalidindi, S.R., 2009. Crystal plasticity simulations using discrete Fourier transforms. *Acta materialia*, *57*(6), pp.1777-1784.

Lu, H. and Wu, C.T., 2006. A grid-based adaptive scheme for the three-dimensional forging and extrusion problems with the EFG method. In *9th International LS-DYNA Users Conference* (Vol. 17, pp. 33-44).

Prithivirajan, V. and Sangid, M.D., 2018. The role of defects and critical pore size analysis in the fatigue response of additively manufactured IN718 via crystal plasticity. *Materials & Design*, *150*, pp.139-153.

Shassere, B., Greeley, D., Okello, A., Kirka, M., Nandwana, P. and Dehoff, R., 2018. Correlation of microstructure to creep response of hot isostatically pressed and aged electron beam melted Inconel 718. *Metallurgical and Materials Transactions A*, *49*(10), pp.5107-5117.

Si, L.Y., Lu, C., Huynh, N.N., Tieu, A.K. and Liu, X.H., 2008. Simulation of rolling behaviour of cubic oriented al single crystal with crystal plasticity FEM. *Journal of Materials Processing Technology*, *201*(1-3), pp.79-84.

Staroselsky, A. and Borkowski, L., 2019. Microstructural Characterization and Simulation of High Temperature Inelastic Deformation and Fracture of Al-Li 2070. *Journal of Materials Engineering and Performance*, *28*(11), pp.6942-6957.

Staroselsky, A. and Cassenti, B.N., 2010. Combined rate-independent plasticity and creep model for single crystal. *Mechanics of materials*, *42*(10), pp.945-959.

Wu, C.T. and Lu, H., Livermore Software Technology Corp, 2010. *Practical fast mesh-free analysis*. U.S. Patent 7,660,480.

Yeratapally, S.R., Glavicic, M.G., Hardy, M. and Sangid, M.D., 2016. Microstructure based fatigue life prediction framework for polycrystalline nickel-base superalloys with emphasis on the role played by twin boundaries in crack initiation. *Acta Materialia*, *107*, pp.152-167.